

Mireille Schneider  
 CPPM, 163, avenue de Luminy, case 907,  
 13288 Marseille cedex 9, France

### Abstract

Recent results on searches for physics beyond the Standard Model obtained by the H1 and ZEUS experiments are reported here. After a brief introduction to the HERA collider, indirect searches for contact interactions and extra-dimensions are presented as well as direct searches for new physics including leptoquarks, lepton-flavour violation, squarks produced by R-parity violation and excited fermions. New results from isolated lepton events and single top searches are also presented. Finally the future prospects of HERA-2 are shown.

## 1 Introduction

HERA is an  $ep$  collider which has especially high sensitivity to new particles coupling to lepton-quark pairs. In 1994-97 HERA collided 27.5 GeV positrons on 820 GeV protons. In 1998 the proton energy was raised to 920 GeV increasing the center-of-mass energy  $\sqrt{s}$  from 300 GeV to 318 GeV. In 1998 and in the first months of 1999, HERA ran with electrons. In May 1999 HERA switched back to  $e^+p$  collisions.

The three main colliding periods as well as the corresponding luminosities for each experiment are summarized in table 1.

Year	Collision	$\sqrt{s}(\text{GeV})$	H1	ZEUS
94-97	$e^+p$	300	36 $\text{pb}^{-1}$	48 $\text{pb}^{-1}$
98-99	$e^-p$	318	14 $\text{pb}^{-1}$	16 $\text{pb}^{-1}$
99-00	$e^+p$	318	65 $\text{pb}^{-1}$	64 $\text{pb}^{-1}$

Table 1: *Luminosities collected by H1 and ZEUS for each colliding period.*

Recent results on searches for new particles based on different models beyond the SM are reported here, as well as searches for rare event topologies with high  $P_T$  leptons and missing momentum.

Several models have been tested analysing the full HERA-1 data corresponding to an integrated luminosity of 115 and 128  $\text{pb}^{-1}$  for H1 and ZEUS respectively.

## 2 Contact Interactions

This indirect search for new processes allows to test the effects of new physics implying the exchange of particles with a mass higher than the center-of-mass energy  $s$ . An effective mass scale  $\Lambda$  is introduced:  $\Lambda \gg \sqrt{s}$ .

Different models beyond the Standard Model (SM) can thus be tested in the frame of contact interactions: for instance, in compositeness models, limits on the mass scale  $\Lambda$  can

be set. Limits on high mass leptoquarks can also be determined via the ratio  $M/\lambda$  where  $\lambda$  is the coupling between leptoquarks and SM particles. Finally results from contact interactions allow also to put limits on the radius of the quark  $R_q$ .

Contact interactions are represented by lagrangian (1) which is added to the SM lagrangian.

$$\mathcal{L}_{CI} = \sum_{a,b=L,R} \eta_{ab}^q (\bar{e}_a \gamma_\mu e_a) (\bar{q}_b \gamma_\mu q_b) \quad (1)$$

$\eta_{ab}^q = \epsilon \frac{g^2}{(\Lambda_{ab}^q)^2}$  are model-dependant coefficients depending on the quark flavour  $q$  and the quark and electron chiralities  $a$  and  $b$ . Different combinations of these coefficients lead to different contact interaction models.  $\epsilon = \pm 1$  is the sign of the interference with respect to the SM,  $\Lambda_{ab}^q$  is the effective mass scale, and  $g$  is the coupling constant, conventionally fixed so that  $g^2 = 4\pi$ .

Contact interactions are searched for by analysing high  $P_T$  samples of deep inelastic scattering candidates (DIS samples). Deviations from the SM in the distributions of usual kinematic variables of the DIS candidates (e.g. the virtuality  $Q^2$  of the exchanged photon) are looked for.

As an example, figure 1 shows a fit of the measured neutral current (NC)  $Q^2$  distribution to the VV compositeness model (this model assumes the same couplings  $\eta_{ab}^q$  for all particle states), in both cases where new physics interferes constructively or destructively with the SM DIS processes. No deviation at high  $Q^2$  is observed, therefore limits are deduced.

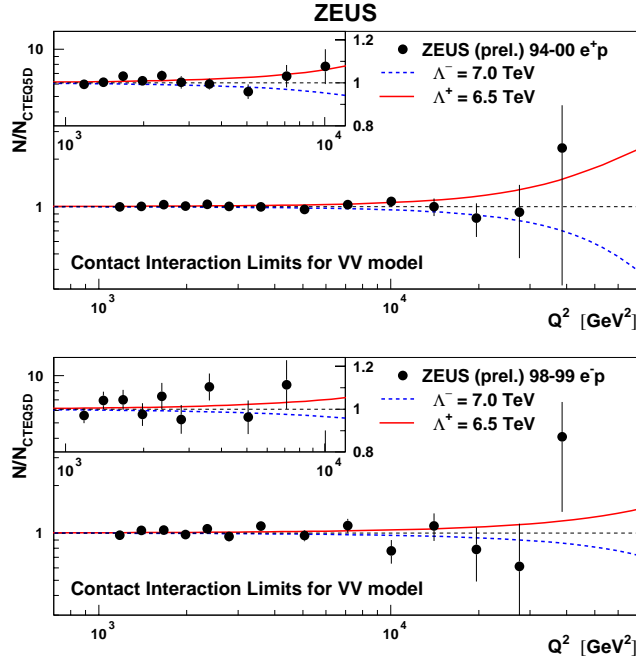


Figure 1: *Ratio between the experimental and SM cross sections as a function of  $Q^2$  according to the VV compositeness model. New physics interferes constructively (solid curve) or destructively (dashed curve) with the SM DIS.*

Figure 2 shows the H1 and ZEUS exclusion limits on the ratio  $\epsilon/\Lambda^2$  for general com-

positeness models [1]. H1 and ZEUS data are in good agreement with the SM expectation.

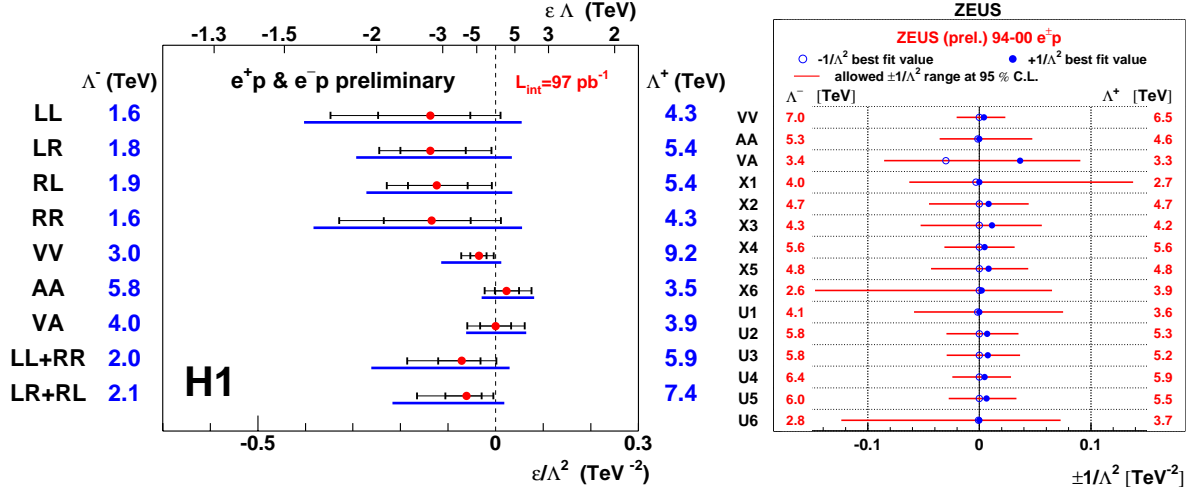


Figure 2: Limits on  $\epsilon/\Lambda^2$  for different compositeness models obtained by H1 and ZEUS. The thick lines in first (second) figure show the H1 (ZEUS) limits on  $\epsilon/\Lambda^2$  analysing 97 (128)  $\text{pb}^{-1}$  of  $e^\pm p$  data. Values outside these regions are excluded at 95% C.L.

The resulting limits on the effective scale  $\Lambda$  are summarized in table 2.

H1	$\Lambda > 1.6 - 9.2 \text{ TeV}$
ZEUS	$\Lambda > 2.6 - 7.0 \text{ TeV}$

Table 2: Limits on the effective mass scale  $\Lambda$  obtained by H1 and ZEUS. The ranges correspond to the different compositeness models.

Measurements of high  $Q^2$  DIS can also be used to set limits on the radius of the quark  $R_q$ : the measurement of the spatial charge distribution of the quark is performed using the classical form factor approximation. In this approximation, the structure of the quark leads to the cross section deviation from the SM presented in equation (2).

$$\frac{d\sigma}{dQ^2} = \frac{d\sigma^{SM}}{dQ^2} \left[ 1 - \frac{R_e^2}{6} Q^2 \right]^2 \cdot \left[ 1 - \frac{R_q^2}{6} Q^2 \right]^2 \quad (2)$$

$R_e$  and  $R_q$  are the root of the mean square radius of the electroweak charge of the electron and the quark respectively.

Assuming that electrons are point-like particles, an upper limit of  $0.73 \cdot 10^{-18} \text{ m}$  is obtained for the quark radius from a fit to the ZEUS data [2].

### 3 Extra-Dimensions

The Large Extra-Dimensions (LED) model, proposed by Arkani-Hamed, Dimopoulos and Dvali assumes a space-time containing  $4+n$  dimensions [3]: the SM particles including the

strong and electroweak bosons are supposed to be confined in a 4D world while gravitons can propagate in  $n$  compactified extra-dimensions.

The effective coupling strength describing the interaction between the gravitons and SM particles is  $1/M_s$ , where  $M_s$  is the fundamental Planck mass scale in the full space. If extra-dimensions are large enough, then  $M_s$  may be in the TeV range. The contribution of graviton exchange to  $eq$  scattering can be described by a contact interaction. Therefore the model is tested using NC samples and fitting the cross section to a formula including the graviton exchange, considering  $M_s$  as a free parameter.

The corresponding limits on the Planck mass scale  $M_s$  for both experiments are summarized in table 3 [2, 4].

	Negative Coupling	Positive Coupling
H1 ( $96 \text{ pb}^{-1}$ )	$M_s^- > 0.93 \text{ TeV}$	$M_s^+ > 0.63 \text{ TeV}$
ZEUS ( $128 \text{ pb}^{-1}$ )	$M_s^- > 0.82 \text{ TeV}$	$M_s^+ > 0.81 \text{ TeV}$

Table 3: *Limits on the Planck mass scale  $M_s$  with H1 and ZEUS detectors.*

## 4 Leptoquarks

In various models (e.g. some models of Grand Unification), triplets of coloured bosons, called leptoquarks (LQs), are supposed to be produced, which could be observed at HERA by an  $eq$  fusion as illustrated in figure 3.

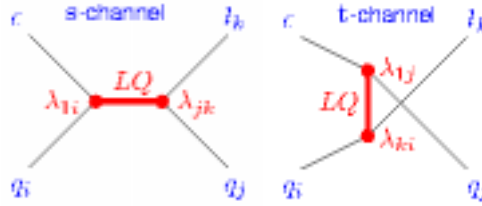


Figure 3: *LQ production (exchange) in the  $s$  ( $t$ ) channel.*

LQs are scalar or vector bosons characterized by a weak Isospin  $T = 0, 1/2, 1$  and a fermionic number  $F = 0, 2$  (defined as  $F = L + 3B$  where  $L$  and  $B$  are respectively the lepton and baryon numbers). The model proposed by Buchmüller, Rückl and Wyler (BRW) [5] describes 14 LQs (each coupling to only one combination of fermion chiralities):

- 7 LQs with a fermion number  $F = 0$  searched for in  $e^+p$  collisions.
- 7 LQs with a fermion number  $|F| = 2$  searched for in  $e^-p$  data.

In the BRW model, first generation LQs decay into  $eq$  and  $\nu q$  with fixed branching ratios.

As the LQs decay topologies are identical to the Deep Inelastic Scattering (DIS) processes, LQs decaying into  $eq$  are searched for in NC samples whereas LQs decaying into  $\nu q$  are searched for in Charged Current (CC) samples.

The presence of LQs would manifest itself as an excess of DIS-like events with a large angle for the final state lepton. Therefore an angular cut varying with the LQ mass is applied in order to optimize the sensitivity to LQs. Mass distributions in the NC and CC channels are respectively shown in figures 4 and 5 [6, 7, 8].

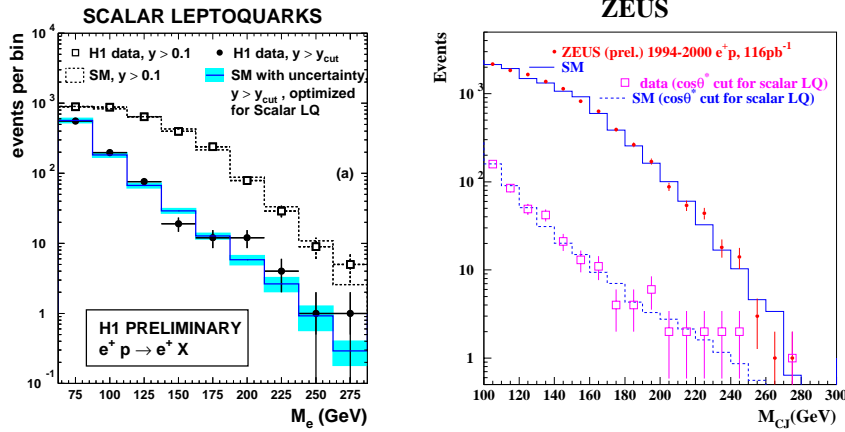


Figure 4: Mass distributions in the NC channel for H1 (left) and ZEUS (right) experiments with 94-00  $e^+p$  data, with and without the angular cut.

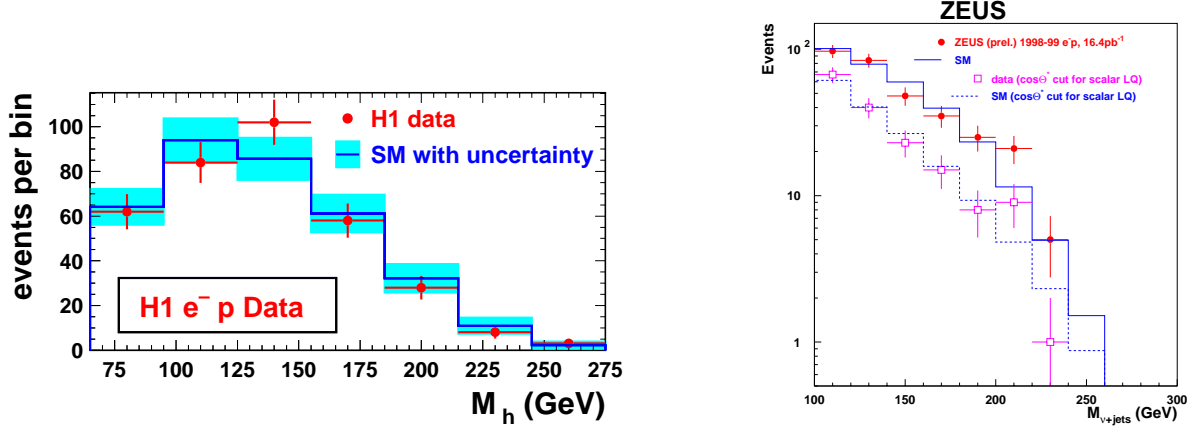


Figure 5: Mass distributions in the CC channel for H1 (left) and ZEUS (right) experiments with 98-99  $e^-p$  data. ZEUS applies an additional angular cut as a function of the LQ mass.

In the NC channel, the previous excess observed at masses around 200 GeV in H1 and ZEUS 1994-97 data has not been confirmed by new 1999-2000 data. Therefore the mass distribution in the full data sample is compatible with the SM expectation. In the CC channel, both experiments show also a good agreement with the SM expectation. Therefore constraints on LQ masses and their coupling  $\lambda$  to  $eq$  pairs are derived.

Figure 6 presents the resulting limits on the coupling  $\lambda$  as a function of the LQ mass for scalar LQs, in the context of the BRW model (fixed branching ratios). HERA limits are seen to be competitive with those obtained at other colliders. Moreover HERA extends the exclusion region at high mass of the LQ.

In the more general case where the branching ratio  $\beta_{eq}$  ( $\beta_{\nu q}$ ) for the LQ decay into  $eq$

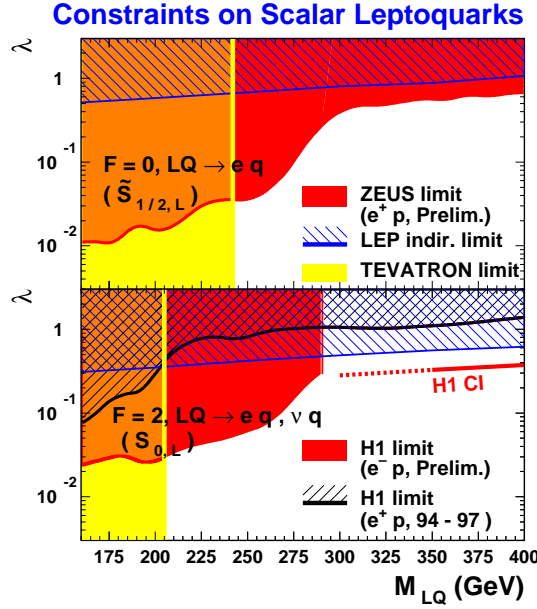


Figure 6: Limits on the coupling  $\lambda$  as a function of the LQ mass for fermion numbers  $F = 0$  and  $F = 2$  for scalar LQs, with HERA, LEP and Tevatron colliders.

$(\nu q)$  is not fixed anymore, constraints on  $\beta_{eq}$  can be set as a function of the LQ mass, for different values of the coupling  $\lambda$ .

H1 results are shown in figure 7 for two example scalar LQs. This shows that HERA limits are compatible with Tevatron for low values of  $\lambda$  and superior at large  $\lambda$ . Moreover HERA extends the limits to small values of  $\beta_{eq}$ .

## 5 Lepton-Flavour Violation

Experiments searching for neutrino oscillations show an increasing evidence for Lepton Flavour Violation, therefore the lepton number is likely to be violated. Processes like  $eq \rightarrow \mu q'$  or  $eq \rightarrow \tau q'$  via a LQ production or exchange are searched for (these processes are also illustrated by figure 3). Both these transitions have been looked for in various data sets, and constraints have been set [9, 10].

As an example, constraints on the process  $eq \rightarrow \mu q'$  which involves two couplings  $\lambda_{eq}$  and  $\lambda_{\mu q}$  are illustrated here.

At low LQ mass, upper limits on the product  $\lambda_{eq} \times \sqrt{BR_{LQ \rightarrow \mu q}}$  can be deduced as a function of the LQ mass. Assuming  $\lambda_{eq} = \lambda_{\mu q}$ , the branching ratio  $BR_{LQ \rightarrow \mu q}$  is fixed to 0.5 and limits on  $\lambda_{eq}$  versus the LQ mass are shown in figure 8 [11]. This figure shows that HERA limits are better than low-energy experiments for  $ed \rightarrow \mu b$  transitions via the process  $B \rightarrow \mu e$  and for a LQ mass lower than 280 GeV.

At high LQ mass, the cross section is proportional to  $\left(\frac{\lambda_{eq}\lambda_{\mu q}}{M^2}\right)^2$  where  $M$  is the LQ mass. Bounds on this ratios were also set in [9] and [10].

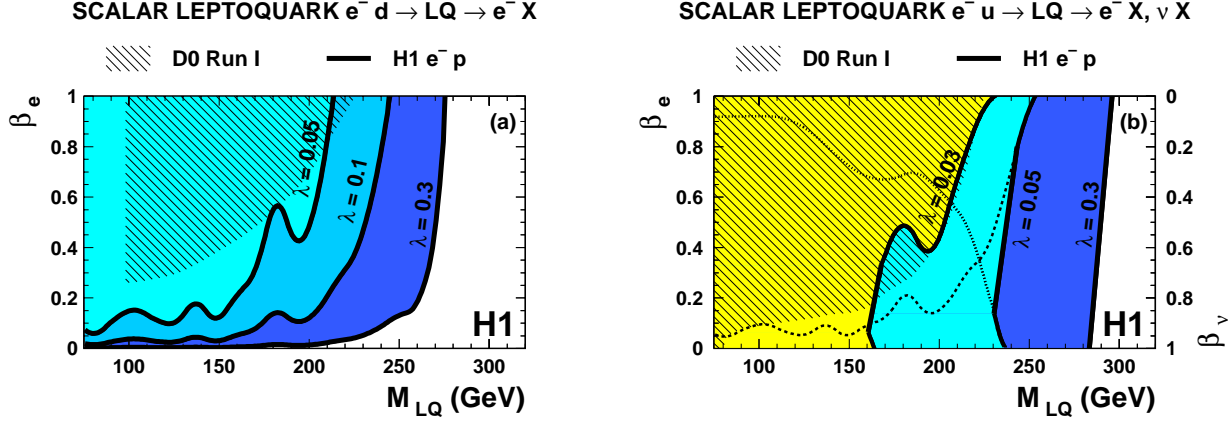


Figure 7: The left (right) plot shows limits on the branching ratio  $\beta_e$  versus the LQ mass for scalar LQs in the NC (NC+CC) channel with H1 data. The hashed region is the region excluded by Tevatron. The domains to the left of the solid curves are excluded by H1. In the second figure, the limits combine the NC and CC channels. For  $\lambda = 0.5$ , the domain excluded by the NC (CC) channel alone is also shown above (below) the dashed (dotted) curve.

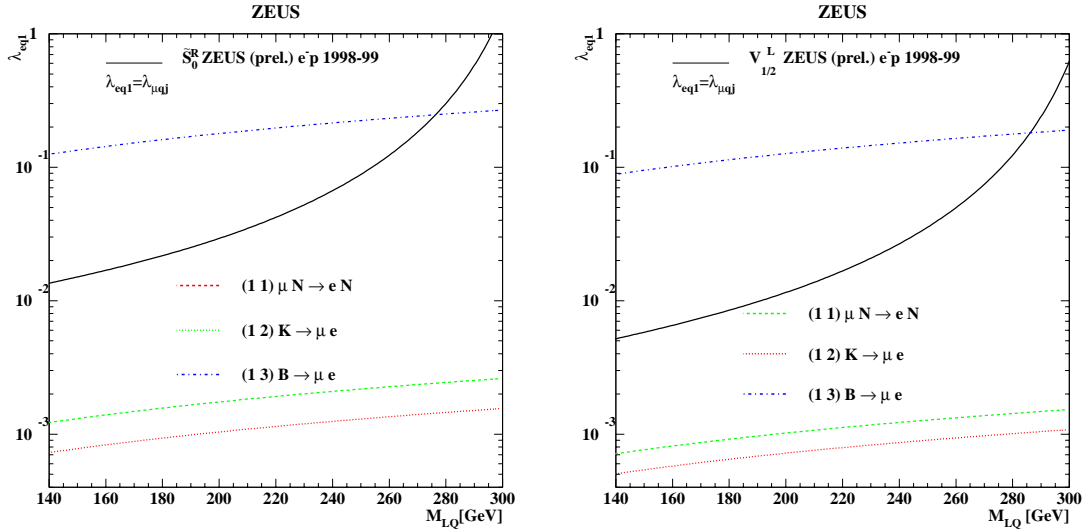


Figure 8: The left (right) plot shows limits on the coupling constant  $\lambda_{eq}$  as a function of the LQ mass for a scalar (vector) LQ exchange from the  $e^-p$  1998-99 ZEUS data.

## 6 Squarks produced by R-parity violation

In the Minimal Supersymmetric Standard Model (MSSM) [12], R-parity is defined as  $R_p = (-1)^{3B+L+2S}$ . SM particles have  $R_p = 1$  whereas their supersymmetric partners have  $R_p = -1$ .

If  $R_p$ -violation would be allowed, superparticles could be produced at HERA by an  $eq$  fusion:  $ep \rightarrow \tilde{q}X$ . This process is illustrated by figure 9. An  $R_p$ -violating coupling  $\lambda'$  is involved corresponding to an  $R_p$ -violation term  $\lambda'_{ijk} L_i Q_j \bar{D}_k$  added to the lagrangian.

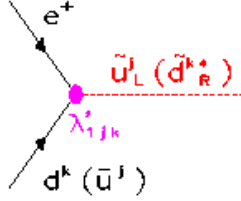


Figure 9: *Squark production at HERA.  $\lambda'$  is the  $R_p$  coupling.*

The  $e^+p$  data can mainly probe the coupling  $\lambda'_{1j1}$  via the process  $e^+ + d \rightarrow \tilde{u}_L$ .

Both decay modes of the squark are investigated at HERA:  $R_p$  decays and “gauge” decays.

The  $R_p$  decay mode is illustrated in figure 10. As the squark can decay into an electron and a quark or a neutrino and a quark, the main backgrounds are respectively NC and CC processes.

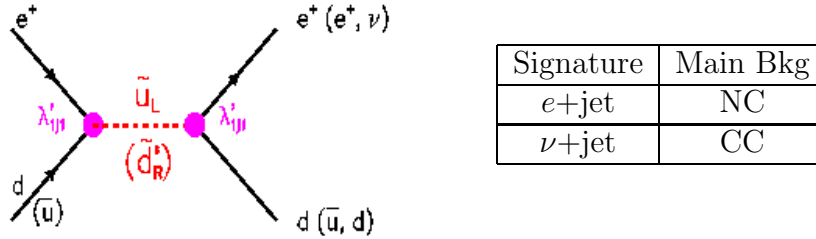
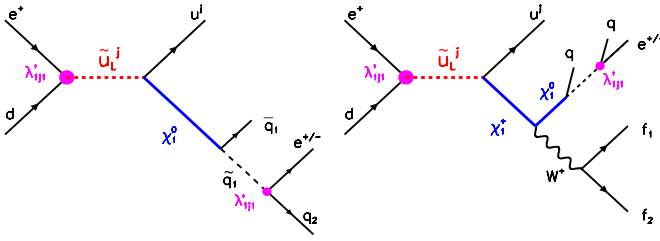


Figure 10: *Squark decay by  $R_p$ -violation and expected signature and main backgrounds from SM processes.*

Example final states resulting from a squark “gauge” decay (mediated by a  $R_p$ -conserving coupling) are illustrated in figure 11. The table indicates all signatures considered, together with their corresponding backgrounds for  $e^+p$  scattering. No deviation from the SM has been observed, therefore limits on the coupling  $\lambda'$  are derived.





Signature	Main Bkg
$e^+ + \text{multi-jets}$	NC
$e^- + \text{multi-jets}$	$\sim$ Bkg Free
$\nu + \text{multi-jets}$	CC
$e + l + \text{multi-jets}$	Small SM Bkg

Figure 11: “Gauge” decay of the squark into a neutralino (left) or chargino (right). When the final lepton (arising from the  $R_p$ -violating neutralino decay) and incident beam lepton have different signs, the channel is almost background-free.

The results have been interpreted in various SUSY models. The first one is the unconstrained MSSM. In this model, sfermion masses are considered as free parameters. The other free parameters are: the squark mass  $M_{\tilde{q}}$ , the soft SUSY breaking mass term  $M_2$ , the mixing mass term for Higgs doublets  $\mu$  and the ratio of the vacuum expectation values of the 2 neutral Higgs bosons  $\tan \beta$ . A scan of the SUSY parameter space ( $M_2, \mu, \tan \beta$ ) is performed. The resulting limits on  $\lambda'$  of the H1 and ZEUS experiments are shown in figure 12 [13, 14].

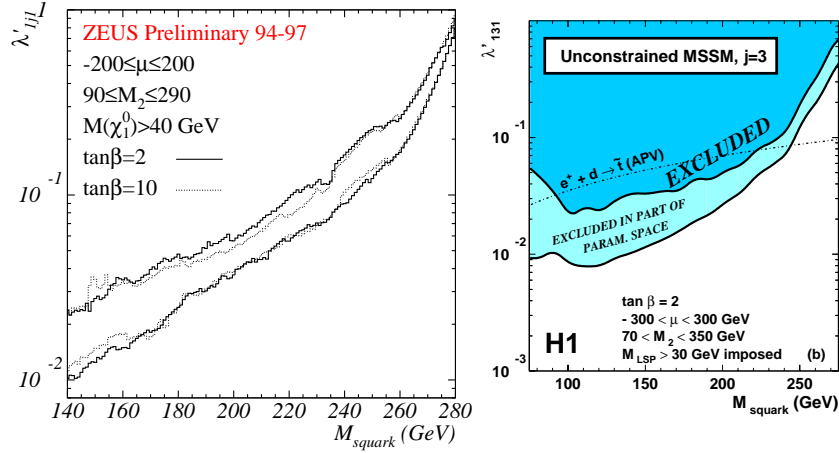


Figure 12: Left (right) plot shows limits on  $\lambda'_{111}$  and  $\lambda'_{121}$  ( $\lambda'_{131}$ ) obtained by the ZEUS (H1) experiment versus the squark mass. The two curves represent for a given value of  $\tan \beta$  the minimum and maximum 95% CL limits obtained when scanning on  $M_2$  and  $\mu$ . In the right plot the colored regions represent the H1 exclusion region while the dashed curve shows the limits from Atomic Parity Violation.

As they are calculated for a large range in  $\mu$  and  $M_2$ , these limits are almost model independent. They are seen to be more restrictive than the indirect bounds from Atomic Parity Violation (APV) for the coupling  $\lambda'_{131}$ , which would lead to stop production at HERA. For a given value of  $\lambda'_{1j1} = 0.3$ , squark masses below 260 GeV are excluded.

Another SUSY model is the minimal Super-Gravity model (mSUGRA) [15] which contains the additional constraint of a universal mass  $m_0$  introduced for all sfermions. In this model the electroweak symmetry breaking is supposed to be driven by radiative

corrections. Therefore the free parameters are mainly  $m_0$  and the unified gaugino mass  $m_{1/2}$  at the GUT scale, the sign of  $\mu$  and  $\tan\beta$ .

The resulting limits in the plane  $(m_0, m_{1/2})$  are presented in figure 13. H1 limits are competitive with (better than) Tevatron for low (medium)  $\tan\beta$ . For the coupling  $\lambda'_{131}$ , H1 bounds are comparable to LEP limits<sup>1</sup> for intermediate values of  $m_0$ ,  $m_{1/2}$  and  $\tan\beta$ .

### Minimal Supergravity + $R_p$ Violation

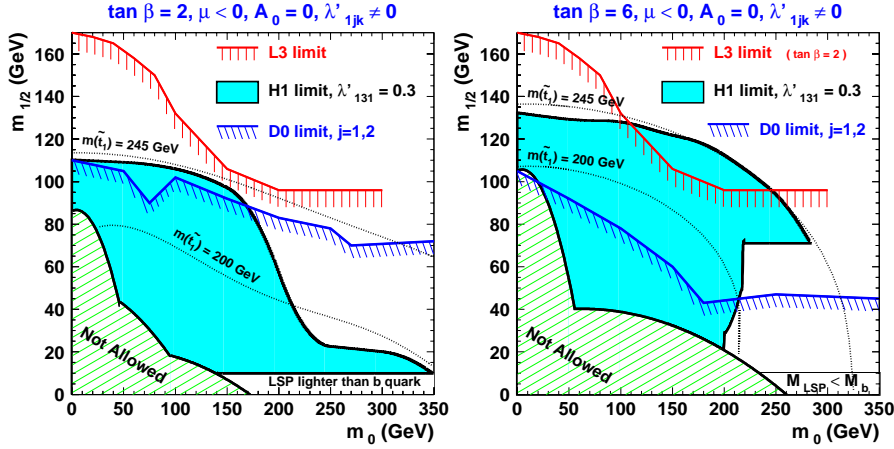


Figure 13: *H1 exclusion regions for a coupling  $\lambda'_{131} = 0.3$  for  $\tan\beta = 2$  (left) and  $\tan\beta = 6$  (right) in the plane  $(m_0, m_{1/2})$ .  $\lambda'_{ijk}$  obtained by D0 and L3 are also shown.*

## 7 Excited fermions

In various extensions of SM, excited states of fermions are expected ( $e^*$ ,  $\nu^*$  and  $q^*$ ). The excited fermions can then de-excite by emission of electroweak bosons  $\gamma$ ,  $Z$  or  $W$  as shown in figure 14 producing various final state topologies to be searched for. This process is described by the effective lagrangian (3) [16].

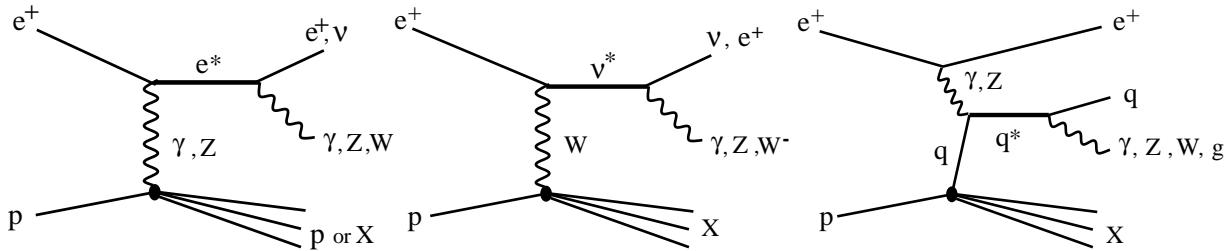


Figure 14: *Excited fermion production at HERA*

<sup>1</sup>LEP limits should not depend too much on  $\tan\beta$  for small and medium values of  $\tan\beta$ .

$$\mathcal{L}_{int} = \frac{1}{2\Lambda} \bar{F}_R^* \sigma^{\mu\nu} \left[ g f \frac{\tau^a}{2} W_{\mu\nu}^a + g' f' \frac{Y}{2} B_{\mu\nu} + g_s f_s \frac{\lambda^a}{2} G_{\mu\nu}^a \right] F_L \quad (3)$$

$F_R^*$  and  $F_L^*$  are the left-handed and right-handed components of the excited form weak isodoublets.  $W_{\mu\nu}^a$ ,  $B_{\mu\nu}$  and  $G_{\mu\nu}^a$  are the field-strength tensors of the respective gauge groups SU(2), U(1) and SU(3).  $g$ ,  $g'$  and  $g_s$  are the SM couplings.  $f$ ,  $f'$  and  $f_s$  determine the coupling strength between the excited fermions and the bosons corresponding to the gauge groups U(1), SU(2) and SU(3).  $\tau^a$  are the Pauli matrices,  $Y$  the weak hypercharge operator,  $\lambda^a$  the Gell-Mann matrices and  $\Lambda$  the compositeness scale.

Assuming relations between  $f$ ,  $f'$  and  $f_s$ , the branching ratios are fixed and limits on the ratio  $f/\Lambda$  versus the excited fermion mass can be deduced from measurements.

Figure 15 shows the mass distribution of the excited electron, neutrino and quark candidates in  $e\gamma$ ,  $eW$  and  $q\gamma$  channels. [17, 18]. No deviation from the SM is observed, therefore limits are established.

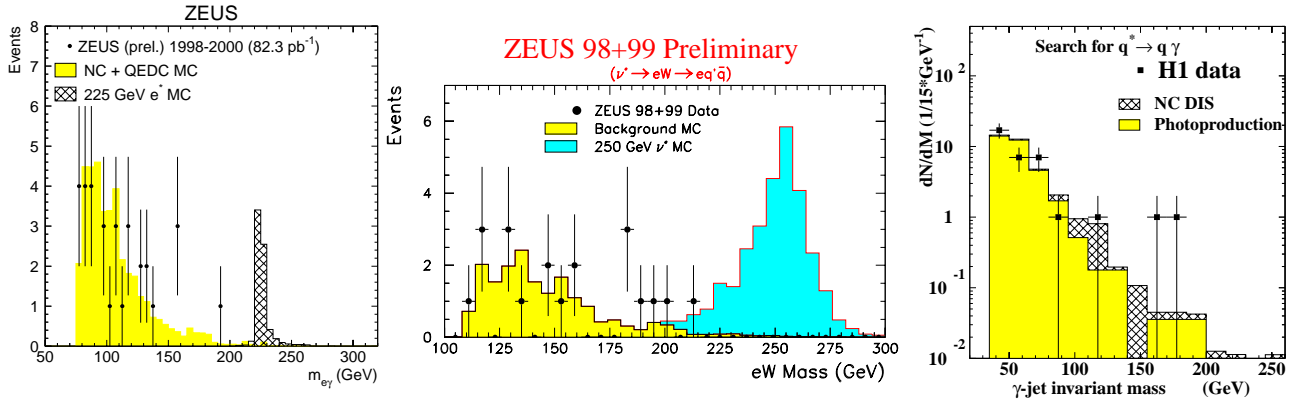


Figure 15: Mass distribution of the  $e^*$ ,  $\nu^*$  and  $q^*$  candidates. Data samples are respectively 98-00  $e^\pm p$  (ZEUS), 98-99  $e^- p$  (ZEUS) and 94-97  $e^+ p$  (H1).

The resulting limits on  $f/\Lambda$  for each channel are presented in figure 16 as a function of the excited fermion mass [19]. In the excited electron channel, HERA limits are competitive with LEP limits for high excited electron masses. In the excited neutrino channel, HERA has a unique sensitivity at high excited neutrino masses. Finally, in the excited quark channel, HERA limits are more sensitive than Tevatron limits if small values of  $f_s$  are considered.

Less model dependent limits are also obtained by allowing an arbitrary ratio  $f'/f$  in the excited neutrino analysis. Figure 17 shows the limits on  $f/\Lambda$  as a function of the ratio  $f'/f$  for different values of the excited neutrino mass. These limits are then converted into limits versus the excited neutrino mass for a range of  $f'/f$  between  $-5$  and  $5$ .

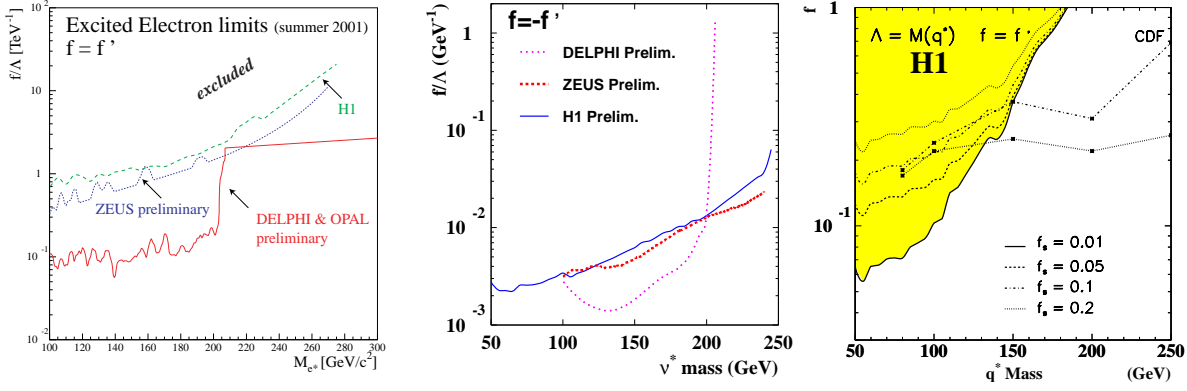


Figure 16: Limits on  $f/\Lambda$  versus the  $e^*$ ,  $\nu^*$  and  $q^*$  mass. The analysed data are respectively 98-00  $e^\pm p$  (ZEUS), 98-99  $e^- p$  (ZEUS and H1) and 94-97  $e^+ p$  (H1). In the  $q^*$  channel, limits are set on  $f$  by fixing  $\Lambda$  to the excited quark mass. Tevatron limits are shown for different values of  $f_s$ .

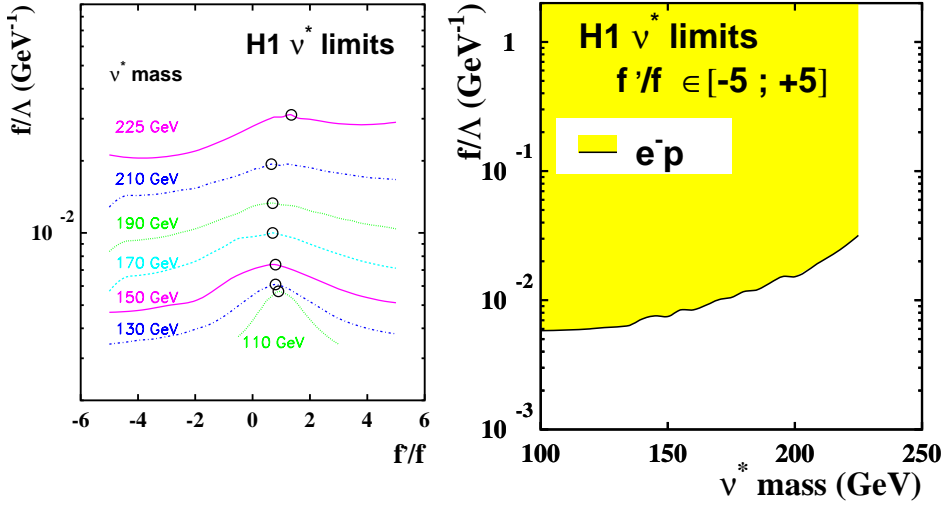


Figure 17: The left plot presents the limits on  $f/\Lambda$  as a function of  $f'/f$  for different values of the excited neutrino mass. The right plot shows the resulting limits on  $f/\Lambda$  as a function of the excited neutrino mass for a range of  $f'/f \in [-5; +5]$ .

## 8 Isolated leptons

High  $P_T$  isolated lepton events with missing  $P_T$  were observed in the 1994-97 H1 data [20]. This analysis has now been extended to the full HERA-1 data. The most likely SM interpretation of these events is W production with a lepton decay of the W as illustrated in figure 18.

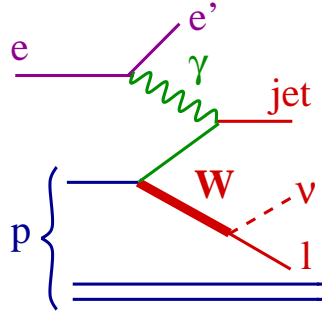


Figure 18:  $W$  production at HERA

The LO cross section of the W production has been calculated and evaluated to be at the level of 1.3 pb. NLO calculations reduce the scale uncertainty to about 10 % at high  $P_T^X$  [21].

W production events are characterized by missing  $P_T$  (due to the presence of the neutrino), a high energy lepton and possibly a jet. The electron and muon channels of the W decay ( $W \rightarrow e\nu$  and  $W \rightarrow \mu\nu$ ) have been analysed by H1 and ZEUS.

Table 4 shows the H1 and ZEUS event rates with the full HERA-1 statistics in both channels as a function of the transverse momentum of the hadronic system  $P_T^X$  [22]. The distribution of the lepton-neutrino transverse mass and the hadronic system transverse momentum  $P_T^X$  are presented in figure 19. At low  $P_T^X$  the observed events are consistent with the SM expectation. However more events than expected are observed by H1 at high  $P_T^X$ .

Data/SM	H1 Prelim. ( $e^+p$ , 102 pb $^{-1}$ )	ZEUS Prelim. ( $e^\pm p$ , 130 pb $^{-1}$ )
$P_T^X > 0$ GeV	18/10.5 $\pm$ 2.5	—
$P_T^X > 25$ GeV	10/2.8 $\pm$ 0.7	2/2.4 $\pm$ 0.2
$P_T^X > 40$ GeV	6/1.0 $\pm$ 0.3	0/1.0 $\pm$ 0.1
	( $e^-p$ , 14 pb $^{-1}$ ) 0/1.8 $\pm$ 0.4	

Table 4: *H1 and ZEUS results (number of data events / MC expectation) in the combined electron and muon channels for the full HERA-1 data sample.*

Figure 20 shows the 2-dimensional ( $P_T^X, M_T$ ) distribution. Few data events are observed in regions where the SM expectation is low. A possible interpretation of these events is the anomalous production of single top events.

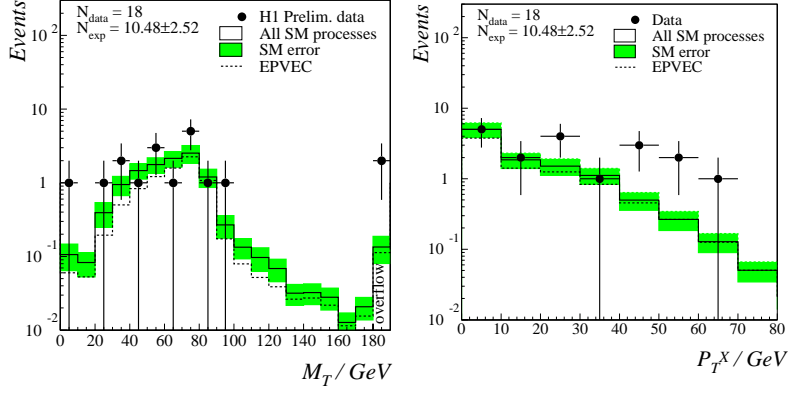


Figure 19: *Distribution of the lepton-neutrino transverse mass  $M_T$  and the hadronic system transverse momentum  $P_T^X$  of the H1 data.*

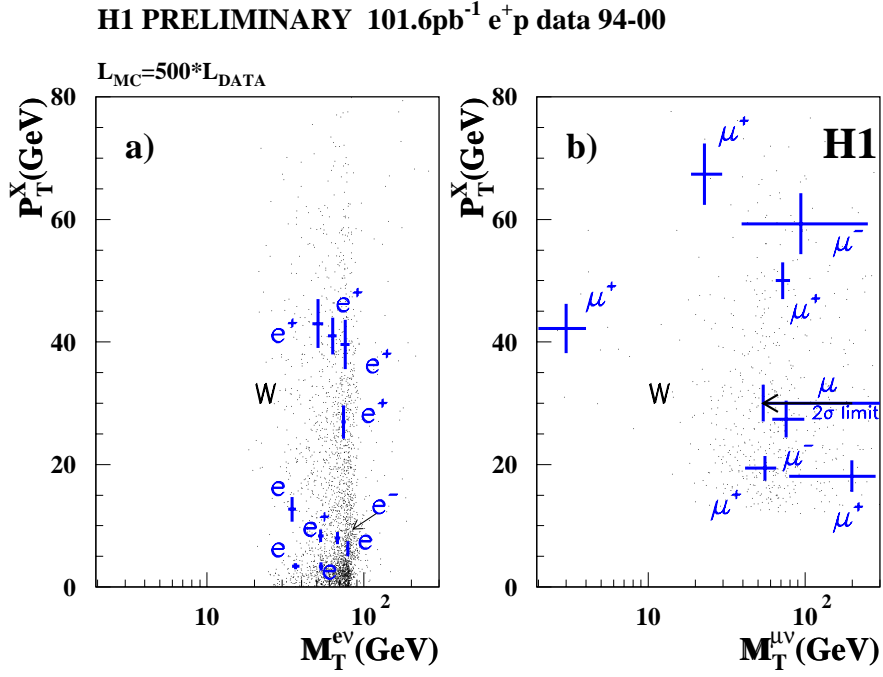


Figure 20: *Hadronic transverse momentum  $P_T^X$  versus the lepton-neutrino transverse mass for electron (left) and muon (right) channels.*

## 9 Single top production

The top quark production within the SM is negligible at HERA. Therefore if any top signal would be found, this would be a sign of new physics. The top quark could be produced by Flavour Changing Neutral Current (FCNC) through a  $\gamma u$  fusion [23]. In the semi-leptonic decay channel ( $t \rightarrow bW$  with  $W \rightarrow l\nu$ ) the final state is composed of an isolated lepton, missing transverse momentum and high hadronic transverse momentum  $P_T^X$ .

The W selection is further tightened in order to select top candidates [24, 25]. Figure 21 presents the resulting mass distribution of the lepton-neutrino-jet system for the electron and muon channels. Several lepton events are in the top mass region.

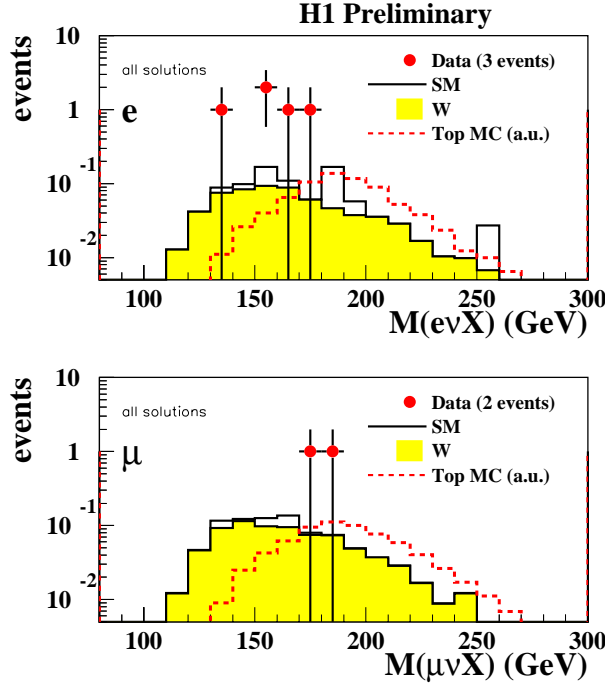


Figure 21: *Mass distribution of the lepton-neutrino-jet system for electron (upper plot) and muon (lower plot) channels. All mass solutions are considered in the  $\nu$  reconstruction.*

A complementary top search has been performed via the hadronic channel ( $t \rightarrow bW$  with  $W \rightarrow q\bar{q}$ ) with three high  $P_T$  jets expected in the final state.

In addition to the existing analysis, further cuts are applied. A 2-jet mass is reconstructed in a W mass window in order to reduce the signal/noise ratio. A 3-jet mass is also reconstructed as shown in figure 22.

The results of the top searches are shown in table 5 for both semi-leptonic and hadronic decay channels. No visible excess is observed in the hadronic channel compared to the SM, therefore limits on anomalous top couplings are derived.

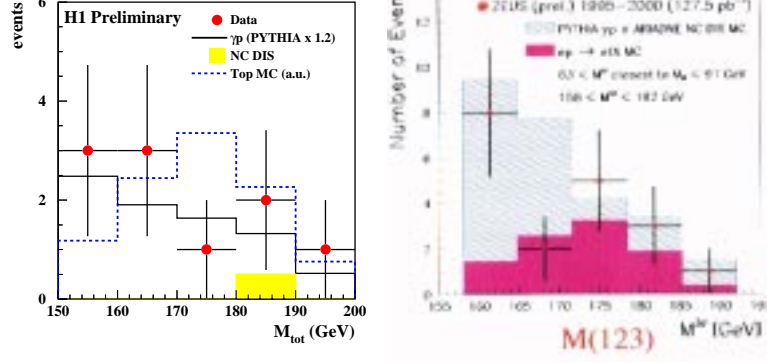


Figure 22: The left (right) figure shows the 3-jet mass distribution of the selected top candidates of the H1 (ZEUS) experiment for a luminosity of  $37 \text{ pb}^{-1}$  ( $128 \text{ pb}^{-1}$ ).

Data/SM	Lepton channel	Hadron channel
H1	$5/1.8 \pm 0.5$	$10/8.3^{+4.2}_{-1.9} \pm 4.2$
ZEUS	0/1.0	19/20.0

Table 5: Single top results (number of data events / MC expectation) in leptonic channel with a luminosity of  $115$  ( $128$ )  $\text{pb}^{-1}$  for H1 (ZEUS), and hadronic channel with a luminosity of  $37$  ( $128$ )  $\text{pb}^{-1}$  for H1 (ZEUS).

HERA resulting limits on  $tu\gamma$  coupling are the following:

- H1:  $\kappa_{tu\gamma} < 0.305$
- ZEUS:  $\kappa_{tu\gamma} < 0.19$

Figure 23 summarizes the limits on the anomalous couplings  $V_Z$  ( $tuZ$  vectorial coupling) and  $\kappa_\gamma$  ( $tu\gamma$  magnetic coupling) obtained at HERA, LEP and Tevatron. HERA sensitivity to  $\kappa_\gamma$  is competitive with other colliders.

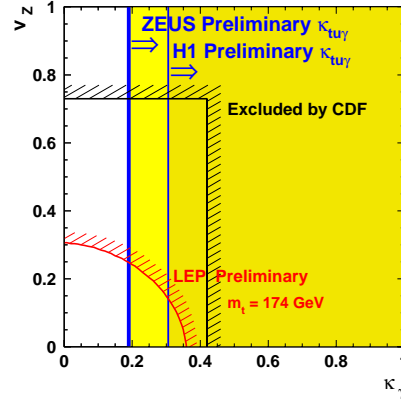


Figure 23: Exclusion region in the plane  $(v_Z, \kappa_\gamma)$ .



## 10 Conclusion and future prospects

HERA is the unique collider to test direct  $eq$  interactions. About  $110 \text{ pb}^{-1}$  of  $e^+p$  data and  $15 \text{ pb}^{-1}$  of  $e^-p$  data have been collected per experiment at HERA-1.

No evidence of new physics has been observed in various models in inclusive analyses (contact interactions, extra-dimensions, leptoquarks) and exclusive analyses (lepton-flavour violation,  $R_p$ -violating SUSY, excited fermions), therefore new constraints have been set. HERA limits are seen to be competitive with and complementary to the LEP and Tevatron searches. The status of isolated lepton events with missing  $P_T$  is still intriguing and will become clearer with the new HERA-2 data.

HERA has been shutdown since fall 2000 for a general upgrade: new focussing magnets have been installed in order to increase the luminosity and many improvements have been performed in the detectors in order to increase their sensitivity. Moreover, the lepton beam will be longitudinally polarised in the H1 and ZEUS interaction regions. The first luminosity runs are predicted for beginning 2002 and HERA-2 is expected to accumulate  $1 \text{ fb}^{-1}$  in the next 5 years. The anticipated factor of ten increase in the integrated luminosity will give an outstanding discovery potential for HERA.

## 11 Acknowledgements

I wish to thank my H1 and ZEUS colleagues who contributed to the results presented here as well as people who helped me in preparing this talk.

## References

- [1] H1 Collab. C. Adloff et al, Phys. Lett. B **479** (2000) 358-370 [hep-ex/0003002]
- [2] ZEUS Collab., EPS 2001 contributed paper, abstract **602**
- [3] N. Arkani-Hamed, S. Dimopoulos and G. Dvali, Phys. Lett. B **429** (1998) 263-272 and Phys. Rev. D **59** (1999) [hep-ph/9803315]
- [4] H1 Collab., ICHEP 2000 contributed paper, abstracts **951, 952**
- [5] W. Buchmüller, R. Rückl and D. Wyler, Phys. Lett. B **191** (1987) 442 and *Erratum* Phys. Lett. B **448** (1999) 320
- [6] H1 Collab., EPS 2001 contributed paper, abstract **822**
- [7] H1 Collab. C. Adloff et al, Phys. Lett. B **523** (2001) 234 [hep-ex/0107038]
- [8] ZEUS Collab., EPS 2001 contributed paper, abstract **600**
- [9] H1 Collab. C. Adloff et al, Eur. Phys. J. C **11** (1999), 447-471 [hep-ex/9907002]
- [10] ZEUS Collab., EPS 1999 contributed paper, abstract **551**
- [11] ZEUS Collab., EPS 2001 contributed paper, abstract **605**
- [12] H. P. Nilles, Phys. Rep. **110** (1984) 1 ; H.E. Haber and G. L. Kane, Phys. Rep. **117** (1985) 75
- [13] H1 Collab. C. Adloff et al, Eur. Phys. J. C **20** (2001) 4, 639-657 [hep-ex/0102050]
- [14] ZEUS Collab., ICHEP 2000 contributed paper, abstract **1042**

- [15] M. Drees and M. M. Nojiri, Nucl. Phys. B **369** (1992) 54 ; H. Baer and X. Tata, Phys. Rev. D **47** (1993) 2739 ; G. L. Kane, C. Kolda, L. Roszkowski and J. D. Wells, Phys. Rev. D **49** (1994) 6173
- [16] K. Hagiwara, S. Komamiya and D. Zeppenfeld, Z. Phys. C **29** (1985) 115
- [17] H1 Collab. C. Adloff et al, Eur. Phys. J. C **17** (2000) 567-581 [hep-ex/0007035]
- [18] ZEUS Collab., EPS 2001 contributed paper, abstract **607**
- [19] H1 Collab., DESY 01-145, Accepted by Physics Letters B, September 2001
- [20] H1 Collab. C. Adloff et al, Eur. Phys. J. C **5** (1998) 575-584 [hep-ex/9806009]
- [21] C. Schwanenberger, talk at DESY 'Workshop Gravity and Particle Physics', "Photoproduction of W bosons at HERA: NLO QCD corrections"
- [22] H1 Collab., EPS 2001 contributed paper, abstract **802**
- [23] T. Han, R.D. Peccei and X. Zhang, Nucl. Phys. B **454** (1995) 527 ; V.F. Obraztsov, S.R. Slabospitsky and O.P. Yushchenko, Phys. Lett. B **426** (1998) 393; T. Han et al., Phys. Rev. D **58** (1998) 073008; T. Han abd J.L. Hewett, Phys. Rev. D **60** (1999) 074015; H. Fritzsch and D. Holtmannspötter, Phys. Lett. B **457** (1999) 186
- [24] H1 Collab., EPS 2001 contributed paper, abstract **824**
- [25] ZEUS Collab., EPS 2001 contributed paper, abstract **650**